High-speed interferometric spectrally encoded flow cytometry

Lior Golan, Daniella Yeheskely-Hayon, Limor Minai, and Dvir Yelin*

Faculty of Biomedical Engineering, Technion—Israel Institute of Technology, Haifa 32000, Israel
**Corresponding author: yelin@bm.technion.ac.il*

Received October 2, 2012; revised November 5, 2012; accepted November 19, 2012;
posted November 20, 2012 (Doc. ID 177046); published December 11, 2012

Spectrally encoded flow cytometry (SEFC) is a promising technique for noninvasive *in vivo* microscopy of blood cells. Here, we introduce a novel SEFC system for label-free confocal imaging of blood cells flowing at velocities of up to 10 mm/s within 65 μm-diameter vessels. The new system employs interferometric Fourier-domain detection and a high-speed wavelength-swept source, allowing 100 kHz line rate, sufficient for sampling the rapidly flowing cells 80 μm below the tissue surface. The large data sets obtained by this technique would improve diagnosis accuracy, reduce imaging time, and open new possibilities for noninvasive monitoring of blood in patients.

OCIS codes: 170.1470, 170.1650.

High-resolution imaging of blood cells in patients is an important challenge in medical diagnosis, potentially offering noninvasive measurement of key blood parameters in real-time, without the pain, overhead cost, and delay associated with the extraction and processing of blood samples. Due to the rapid flow of the blood cells, high-resolution imaging techniques such as laser-scanning confocal microscopy [1] and photoacoustic microscopy [2] are often ineffective. Unfortunately, faster imaging methods such as, ultrasound [3], laser speckle imaging [4], and Doppler optical coherence tomography [5], lack sufficient resolution for imaging subcellular features within the blood stream. Using fluorescence confocal microscopy, which was specifically adapted for *in vivo* flow cytometry (IVFC), characterization of large populations of cells was demonstrated in animal models without blood extraction [6]. Adaptation of IVFC for clinical use in human patients requires, however, injection of fluorescent markers into the blood, which prevents safe clinical implementation of the technique.

Recently, a technique termed spectrally encoded flow cytometry (SEFC) was demonstrated [7,8] using broadband light, a single-mode fiber, and spectrally dispersive optics for high-resolution imaging of unlabeled blood cells flowing inside the human body. In SEFC, a variant of spectrally encoded confocal microscopy [9,10], one axis is encoded by wavelength, while the other is encoded by time, utilizing the nearly linear motion of the flowing cells crossing the spectral line for 2D confocal imaging. An important limitation of the previously demonstrated SEFC system [8] was associated with the limited imaging rate (1.3 kHz) of its high-sensitivity EMCCD camera, enabling resolving cells flowing at up to approximately 1.5 mm/s; cells flowing at higher speed, such as those within large capillary vessels, would appear undersampled, preventing sufficient data points for effectively extracting important cellular features.

Here, we demonstrate an SEFC system capable of high-resolution imaging of cells flowing at speed of up to 10 mm/s across vessels of several tens of micrometers in diameter. Using a wavelength swept source at 100 kHz sweep rate [11], a Mach–Zender interferometer configuration, and Fourier-domain detection [12], we achieve a 70-fold improvement in imaging speed, allowing imaging cells in vessels 65 μm in diameter, located 80 μm below the tissue surface.

Our high-speed SEFC system, schematically illustrated in Fig. 1, used light from a 100 kHz wavelength-swept source (SSOCT-1060, Axsun Technologies, 1060 nm center wavelength, 110 nm sweep range, 15 mW output power), which was coupled into the input port of a fiber-optic Mach–Zender interferometer. The imaging probe, located at the sample arm of the interferometer consisted of a collimating 40 mm focal length lens (resulting in a 7 mm beam diameter), a transmission diffraction grating (600 l/mm, Wasatch photonics), and a relay telescopic arrangement comprised of two achromatic lenses (50 mm focal length) that imaged the field at the grating onto the back aperture of a high-numerical aperture objective lens. At the reference arm of the interferometer, the optical path length was adjusted to match that of the imaging plane using a corner reflector mounted on a linear translation stage. The interference between the imaging and reference signals was recorded using a balanced detector after a 50:50 fiber coupler, and sampled using a 12 bit analog-to-digital converter (ADC) at a rate of 310 Mhz. Data from the ADC was analyzed by a computer and displayed as a continuous 2D time-wavelength (space) image.

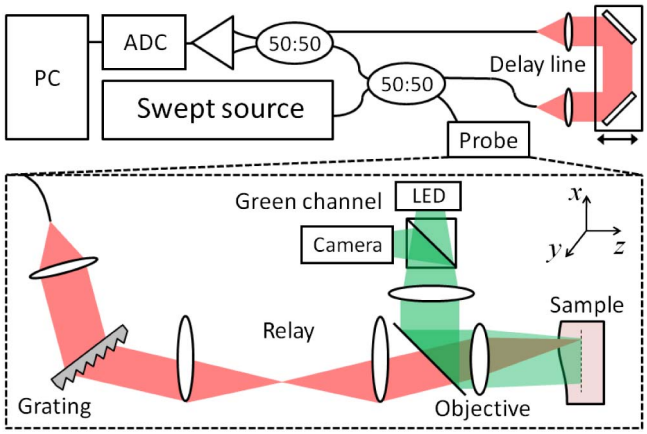

Fig. 1. (Color online) SEFC system layout.

Data acquisition and processing is demonstrated (Fig. 2) by imaging a reflective resolution target, which was linearly translated across the imaging line using a 20×, NA = 0.4 objective lens (Olympus). As wavelength is scanned, the focused beam effectively scans a lateral line on the sample, while the reflected light interferes with the reference light on the detector, generating a signal proportional to the sample reflectivity modulated by a carrier frequency determined by the path length difference between the interferometer arms [Fig. 2(a), solid curve].

In order to extract the reflectivity envelope from the raw data, the magnitude of the analytical continuation of the signal was calculated using a discrete Hilbert transform [13] [Fig. 2(a), dashed curve]. The modulation with a carrier frequency modifies the signal spectrum, effectively doubling the signal bandwidth [Fig. 2(b)]. To avoid aliasing, the signal bandwidth must not exceed half the sampling frequency F, limiting the wavelength sweep velocity v_{sweep} to:

$$v_{\text{sweep}} < \frac{F \cdot \delta x}{4},$$

where δx denotes the lateral optical resolution. Optimally, $v_{\text{sweep}} = F \cdot \delta x/4$, and the modulation frequency $v_m = F/4$ [14]. A complete two-dimensional (2D) raw data of the resolution target [Fig. 2(c)] was obtained by moving the target in the Y-axis at a speed of 50 mm/s, corresponding to an effective image rate of 100 frames (1000 lines) per second. The total time required for computing the reflectivity image [Fig. 2(d)] was approximately 0.3 s on a standard PC, potentially allowing real-time display rates of 1.6 frames/s.

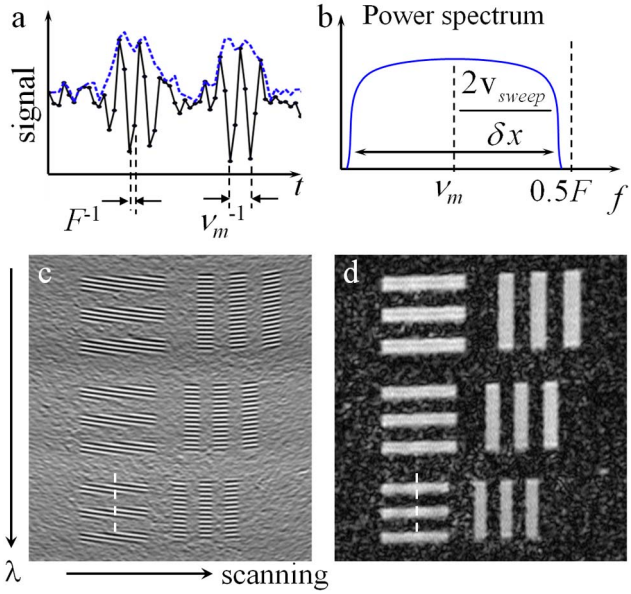

Fig. 2. (Color online) (a) Intensity profiles obtained from a resolution target before (solid curve) and after demodulation (dashed curve). Circle markers indicate sampling points, (b) schematic illustration of the power spectrum of a modulated signal, (c) 2D SEFC raw (before demodulation) image of a resolution target scanned at 50 mm/s, (d) demodulated image using discrete Hilbert transform. Dashed white lines in (c) and (d) indicate the location of the signal profile in (a).

Imaging of rapidly flowing blood cells was demonstrated using a high numerical aperture water-immersion objective lens (1.2 NA, 60×, Olympus), providing lateral and axial resolutions of approximately 0.6 μm (edge response, FWHM) and 1.1 μm (z-scan, FWHM), respectively. The lateral resolution was somewhat lower than theoretically predicted (0.35 μm, FWHM), presumably due to optical aberrations of the objective lens, which was optimized for the visible wavelength range. Detection sensitivity (ratio between maximum signal and noise floor) was approximately 35 dB. A syringe pump and a rectangular 5 mm × 0.8 mm transparent flow chamber were used for generating *in vitro* flow of diluted blood (1∶10 in phosphate-buffered saline with 2% bovine serum albumin) at 8 ml/ min. Blood cells were clearly visible in the SEFC images (Fig. 3), having similar appearance (smooth round red cells, larger speckled white cells) to blood cells in previously reported images [8] that were acquired at considerably lower flow speeds.

In order to demonstrate *in vivo* imaging of blood cells flowing within large capillaries, the lower lip of a volunteer was pressed against a cover slip attached to a protective aluminum cap, and was kept still for a duration of several seconds. Controlling the exact imaging depth was achieved by varying the (water-filled) gap between the objective lens and the cover glass using custom-built small-pitch threaded objective mount. Identification of deep capillaries and fine positioning of the SEFC field-of-view was assisted by an auxiliary wide-field imaging channel [8], using a green (520 nm wavelength) LED, a long-pass dichroic mirror (680 nm cut-on wavelength), a video-rate monochrome camera (UI-2220, IDS), and a pair of crossed polarizers for rejecting surface reflections.

A 65 μm blood vessel, located approximately 80 μm under the surface of the oral mucosa of a volunteer, was imaged by our old noninterferometric system (800 nm center wavelength, 1.3 kHz line rate) [8] [Fig. 4(a)], and by our new interferometric swept source system (1060 nm center wavelength) at 100 kHz line rate [Fig. 4(b)]. The nearly two-orders of magnitude improvement in temporal resolution reveal a dramatic improvement of image resolution in the time axis, enabling the imaging of cells flowing at approximate speed of 10 mm/s and determining their shapes in physiological conditions. In general, the relatively rigid white blood cells (WBCs) [Fig. 4(c)] have appeared to retain their general shape during rapid flow, resembling their *in vitro*

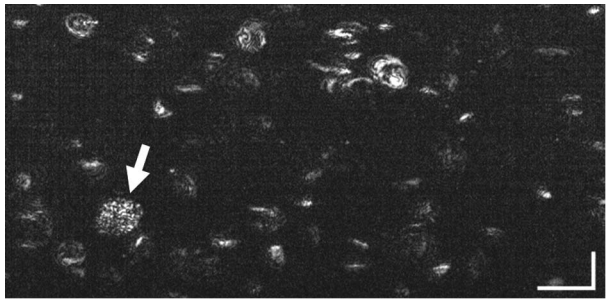

Fig. 3. *In vitro* high-speed SEFC image of diluted whole blood. A white blood cell flowing at 12 mm/s is marked by an arrow. Horizontal scale bar, 1 ms; vertical scale bar, 10 um.

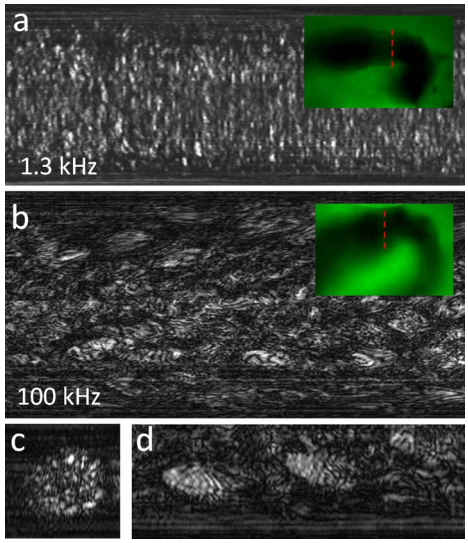

Fig. 4. (Color online) (a) *In vivo* SEFC image of cells flowing within a 65 μm diameter vessel, acquired using a broadband source at 1.3 kHz line rate acquisition, (b) SEFC image of the same vessel (at slightly different location) captured using Fourier-domain interferometry and a wavelength-swept source at 100 kHz line rate. Insets: green widefield images of the vessel; dashed red lines mark the position of the spectrally encoded imaging lines in (a)–(c). *In vivo* imaging of a white blood cell flowing at 4.5 mm/s. (d) *In vivo* imaging of slipper-shaped red blood cells flowing at 7 mm/s.

appearance (Fig. 3), while some red blood cells (RBCs) [Fig. 4(d)] exhibited various deformed shapes under physiological shear stress conditions, including slipper-like shapes [15] near the vessel wall, which resulted in images with a sharp, rounded leading edge and a broader trailing edge.

Typical blood flow velocities in the microcirculation could reach tens of mm/s [16], and while our previous work have shown clear images of blood cells flowing at 1–2 mm/s, at least an order of magnitude improvement in imaging rate is required for *in vivo* measurement of blood cell properties in most accessible vessels. Thanks to the high wavelength sweep rate of our light source and the high sensitivity of heterodyne detection, cells flowing at speeds of up to 10 mm/s could be adequately sampled along the flow axis. Such imaging speed now allows us to image cells within large diameter vessels, which could significantly improve the quality of the acquired data. For example, counting and identifying a specific type of WBCs requires screening of large volumes of blood for achieving sufficient cell-count rates of high statistical significance. In addition, determining hematocrit levels at sufficient accuracy may require imaging of blood cells close to the vessel centerline, where their velocity is maximal [17].

There are some challenges associated with imaging within large vessels, perhaps the most important is the reduced image quality caused by the optical (mainly forward) scattering induced by the layers of RBCs near the front vessel wall. These aberrations may cause cells crossing the focal line to appear with irregular speckled appearance [see Fig. 4(b)]. Another difficulty in imaging inside large vessels is handling the large quantities of raw data: nearly 270 megabyte of data was captured each second, requiring high-speed data storage and dedicated software for real-time display. With the new system, thanks to the high sensitivity and slightly longer wavelength, which is scattered less by the tissue, we have managed to image vessels as deep as 100 μm below the tissue surface, limited only by the high scattering of the mucous membrane.

In summary, Fourier-domain interferometric SEFC was presented, allowing high throughput confocal imaging of blood cells flowing at physiological velocities within large capillary vessels. The system was demonstrated by imaging blood cells at subcellular resolution within 65 μm diameter capillaries located approximately 80 μm below the tissue surface. The new system represents significant improvements in several key imaging parameters over previous systems [7,8], including imaging speed, sensitivity, and penetration depth. Using a robust fiber-optic based configuration and a probe that is insensitive to back-reflections, the system's reliability and portability has been significantly improved, potentially allowing the measurement of key blood parameters using a noninvasive, clinically viable system.

References

1. T. Wilson, ed., *Confocal Microscopy* (Academic, 1990).
2. L. V. Wang, Nat. Photonics **3**, 503 (2009).
3. J. V. Chapman, *Noninvasive Evaluation of Hemodynamics in Congenital Heart Disease* (Kluwer, 1990).
4. A. F. Fercher and J. D. Briers, Opt. Commun. **37**, 326 (1981).
5. Z. Chen, T. E. Milner, S. Srinivas, X. Wang, A. Malekafzali, M. J. C. van Gemert, and J. S. Nelson, Opt. Lett. **22**, 1119 (1997).
6. J. Novak, I. Georgakoudi, X. Wei, A. Prossin, and C. P. Lin, Opt. Lett. **29**, 77 (2004).
7. L. Golan and D. Yelin, Opt. Lett. **35**, 2218 (2010).
8. L. Golan, D. Yeheskely-Hayon, L. Minai, E. J. Dann, and D. Yelin, Biomed. Opt. Express **3**, 1455 (2012).
9. G. J. Tearney, R. H. Webb, and B. E. Bouma, Opt. Lett. **23**, 1152 (1998).
10. C. Boudoux, S. Yun, W. Oh, W. White, N. Iftimia, M. Shishkov, B. Bouma, and G. Tearney, Opt. Express **13**, 8214 (2005).
11. R. Huber, M. Wojtkowski, and J. G. Fujimoto, Opt. Express **14**, 3225 (2006).
12. D. Yelin, W. M. White, J. T. Motz, S. H. Yun, B. E. Bouma, and G. J. Tearney, Opt. Express **15**, 2432 (2007).
13. S. S. C. Chim and G. S. Kino, Appl. Opt. **31**, 2550 (1992).
14. K. G. Larkin, J. Opt. Soc. Am. A **13**, 832 (1996).
15. R. Skalak and P. I. Branemark, Science **164**, 717 (1969).
16. A. C. Burton, *Phyisiology and Biophyisics of the Circulation*, 2nd ed. (Year Book Medical Publishers, Inc., 1972).
17. S. Kim, R. L. Kong, A. S. Popel, M. Intaglietta, and P. C. Johnson, Am. J. Physiol. **293**, H1526 (2007).